



projector augmented wave (PAW) implementation in the VASP code [5]. The details of the present approach are described in Refs. [6,7].

To study the *generic tendency* of  $\text{Zn}_x\text{Cu}_{4-x}\text{X}$  towards doping, independent of the specific dopant chemistry or whether the doped impurity is fully ionized or not, we study a model of “non-chemical doping” (analogous to gating) whereby extra “doped electrons” are added to the host crystal supercell (with a compensating positive background to assure electro-neutrality) while allowing the atoms and all electrons to self-consistently seek the new low-energy configurations. Generally, the localization of charge carriers requires an initial structural perturbation in order to break the symmetry and trigger the polaronic trapping; otherwise the lattice relaxation will end up in a local minimum with the free (delocalized) charge carrier. Our initial nudge is to elongate the 4 Cu-O bonds in one  $\text{CuO}_4$  plane non-equivalently by  $\sim 10\%$  and then relax the atomic positions to see if such a local symmetry breaking will stay.

Having successfully predicted a number of dopant behaviors (either polaron or extended state being the ground state) [8-10], the onsite potential approach provides us more insight on how the localization picture is related to the correction of non-linearity. For the onsite electron potential method, we add electron potentials on certain  $lm$  decomposed orbitals on top of the DFT+U framework, in which the Dudarev’s approach [11] is used for Cu-d and Zn-d states, i.e.,  $(U-J)_{\text{Cu}} = 5$  eV and  $(U-J)_{\text{Zn}} = 6$  eV, respectively. We also added a non-local external potential (NLEP)  $V_{\text{O,p}} = -1$  eV on O-p orbitals for the empirical band-gap correction [12]. The onsite potential is implemented as the combination of DFT+U and NLEP method electron doping, the

rrpocmialgslctryrbstatep

dielectric constant that enters into the image charge corrections, our calculated electronic contribution to the static dielectric constant by DFT+U is about 3.56, based on the real part of the dielectric function  $\epsilon_1(\omega)$  for  $\omega = 0$ . The ionic contribution is calculated using density-functional perturbation theory [14]. The total dielectric constants of kagomé  $\text{ZnCu}_3(\text{OH})_6\text{BrF}$  are thus 7.75.

## Section II. Calculated exchange-interaction parameters and doping effects of antiferromagnetic $\text{ZnCu}_3(\text{OH})_6\text{BrF}$

The exchange-interaction parameters are determined by comparing total energy of different magnetic configurations obtained from DFT calculations. In a  $2 \times 2 \times 1$  supercell (24 Cu atoms), we consider four kinds of exchange interactions for simplicity, including three intralayer interactions  $J_1, J_2, J_d$  and one interlayer interaction  $J_i$ , as indicated in Fig. S1. According to Heisenberg Hamiltonian model, the total energy of a specific magnetic configuration can be written as:

$$E = - \sum_{\langle ij \rangle} J_{ij} \mathbf{S}_i \cdot \mathbf{S}_j, \quad (\text{S1})$$

where,  $\mathbf{S}_i$  denotes spin orientation. Table SI summarizes the exchange-interaction parameters of  $\text{ZnCu}_3(\text{OH})_6$

incorporated. Studying coupling of different magnetic order is possible but outside the scope of this paper.

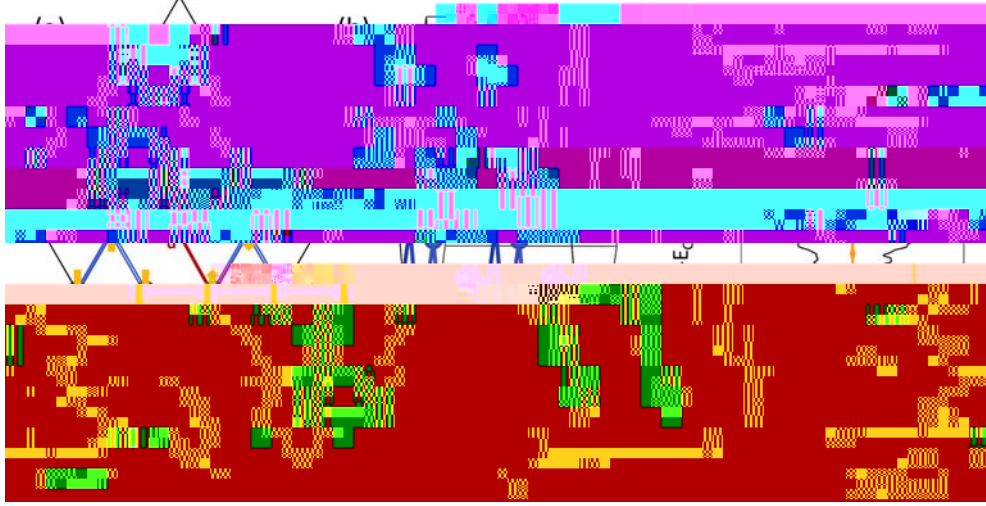


Fig. S1: (a,b) Kagome lattice of copper atoms in  $\text{ZnCu}_3(\text{OH})_6\text{BrF}$ , with the exchange-interaction parameters indicated by solid (intralayer interaction) and dashed lines (interlayer interaction), respectively. (c) Calculated total density of states (DOS, black) and projected DOS of  $\text{Cu}^{1+}$  ion (orange) for doping 1 electron into a 24-atom supercell ( $1/3$  e/Cu). The magnetic configuration has the lowest energy among the five configurations considered, with the spin orientations indicated by the orange arrows in panel (a).

Table SI: Exchange-interaction parameters of  $\text{ZnCu}_3(\text{OH})_6\text{BrF}$ .

Name	$d_{\text{Cu-Cu}}$ ( $\text{\AA}$ )	Exchange interaction (meV)
$J_1$	3.28	47.8
$J_2$	5.68	0.8
$J_d$	6.55	-0.3
$J_{int}$	4.57	1.7

### Section III. Calculated polaron states of various electron-doped systems

To simulate a higher doping concentration, we add one electron non-chemically into a unit cell with 6 Cu atoms (corresponding to a concentration of 16.7% per Cu). The calculated DOS of electron doped  $\text{ZnCu}_3(\text{OH})_6\text{BrF}$  is shown in Fig. S2. We find that this Cu  $d^{10}$  states is still localized inside the band gap. Thus, we estimate that the electron polaron nature of kagome compound  $\text{ZnCu}_3(\text{OH})_6\text{BrF}$  is independent on different concentrations we considered.

Fig. S2: (a) Calculated total density of states (DOS, black) and projected DOS of  $\text{Cu}^{1+}$  ion (orange) by hybrid functional (HSE06) for doping 1 electron non-chemically into a unit cell (1/6 electron per Cu). (b) Charge density of the highest occupied states (black

and  $\text{Cu}^{2+}$ -OH coordination are robust with the presence of small symmetry breaking distortions.

Fig. S3: Calculated total density of states (DOS, black) and projected DOS of  $\text{Cu}^{1+}$  ion

PBE+U level [(U-J)<sub>Cu</sub> = 5 eV and NLEP V<sub>O,p</sub> = -1 eV] produces the band gap to be 0.81 eV.

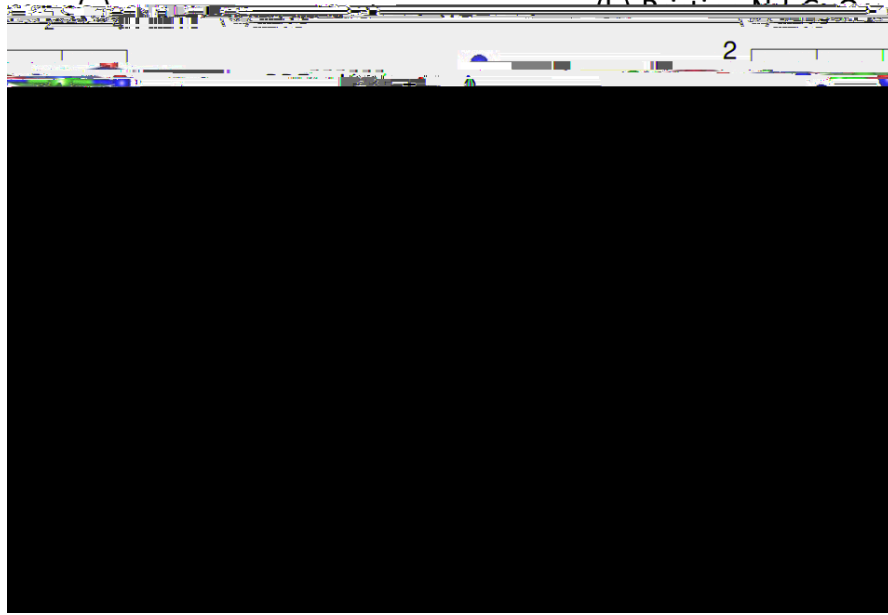


Fig. S4: (a) Crystal structure of  $T'$  Nd<sub>2</sub>CuO<sub>4</sub>. Nd, Cu and O atoms are indicated by green, blue and red balls, respectively. (b) Calculated total density of states (DOS, black) for pristine Nd<sub>2</sub>CuO<sub>4</sub>. The origin and blue curves denote the projected DOS of Cu and O atoms, respectively.

**Electron doped  $T'$  Nd<sub>2</sub>CuO<sub>4</sub>:** To obtain carrier concentration comparable to experiments, we construct a  $2 \times 2 \times 1$  supercell containing 32 Nd, 16 Cu and 64 O atoms. Firstly, we add one electron to the system. The resulting doping concentration is 6.25% per f.u.. According to our calculations, structure with local distortion is energetically more favorable than the symmetry structure by 13 meV/Cu. In the distorted structure, four Cu-O bonds are elongated by 0.11 Å (from 1.97 to 2.08 Å) simultaneously. Projected DOS plot (Fig. S5a) and polaron charge density (Fig. S5b) indicate that the added one electron forming a polaron with diameter about 6.8 Å (Fig. S5c), distributing on the Cu<sup>1+</sup> ion and its surrounding O ligands. Additionally, the adding electron narrows the band gap to 0.57 eV. Our results show good consistent with the transport measurements, i.e., at relatively low doping concentration,  $T'$ -NCO remains

semiconducting [18,19]. However, taking the larger polaron size and narrowing band gap into consideration, it is reasonable to predict that  $T'$ -NCO may be conductive at a moderate doping concentration.

Fig. S5: (a) Calculated total DOS (black) and projected DOS of Cu (origin) and O (blue) for  $\text{Nd}_2$



respectively. On the other hand, SNN turned out to be metallic. Projected DOS (Fig. S6a and S6b) and partial charge density (Fig. S6c and S6d) indicate that the new valence band maximum is mainly distributed by two Cu and coordinated O atoms, similar to one electron doping situation (Fig. S5a and S5b). Considering the tiny band gaps and substantial polarons overlaps, NN and TNN are readily to be conductive due to polaron hopping. Thus, our calculations are consistent with experimental results that  $T'$  NCO undergoes semiconductor-metal/superconductor transition at relatively high doping concentration [18,19].

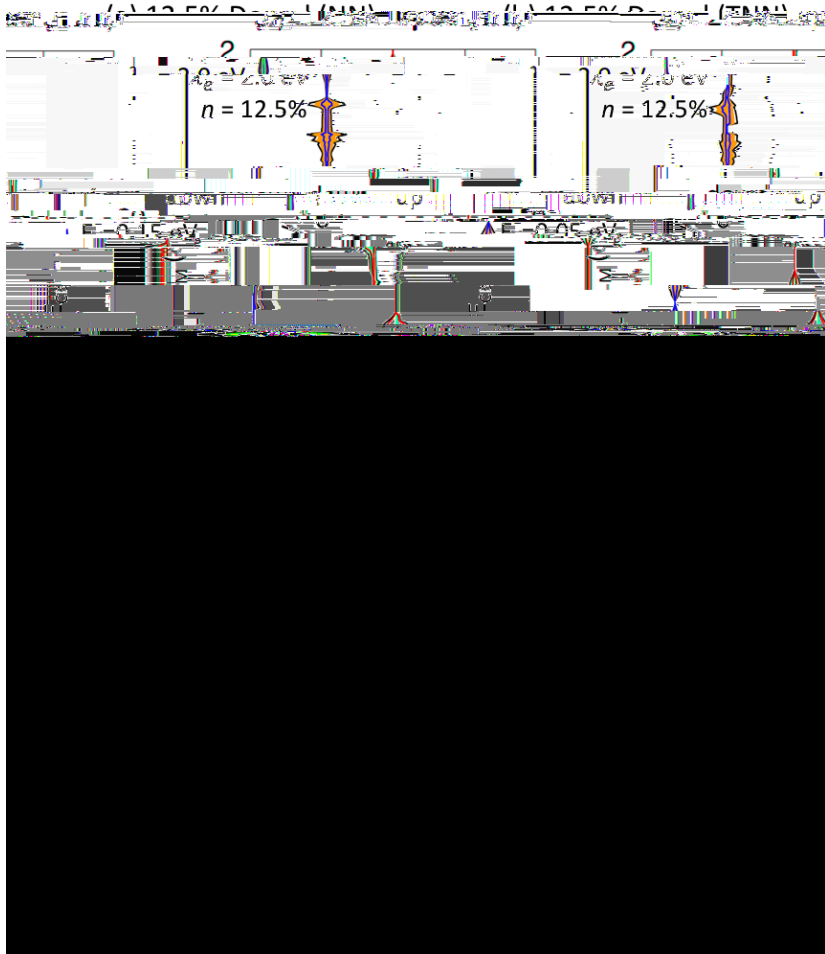


Fig. S6: Calculated total DOS (black) and projected DOS of Cu (origin) and O (blue) for  $0.125 e^-/\text{Cu}$  doped  $\text{Nd}_2\text{CuO}_4$  with (a) NN and (b) TNN configurations. Onsite potential for CONL correction is 2 eV. Highest occupied states charge density of the  $0.125 e^-/\text{Cu}$

doped  $\text{Nd}_2\text{CuO}_4$  with (c) NN and (d) TNN configurations. The light green circles denote polarons distributing on Cu and coordinated O ligands.

Table SII: Relative energies and band gaps of 12.5% electron-doped  $\text{Nd}_2\text{CuO}_4$  with NN, SNN and TNN configurations

Configuration	Relative Energy (meV/Cu)	Band Gap (eV)
NN	4	0.05
SNN	6	Metallic
TNN	0	0.15

## References

- [1] G. Kresse and D. Joubert, *Phys. Rev. B* **59**, 1758 (1999).
- [2] G. Kresse and J. Furthmüller, *Comp. Mater. Sci.* **6**, 15 (1996).
- [3] J. P. Perdew, K. Burke, and M. Ernzerhof, *Phys. Rev. Lett.* **77**, 3865 (1996).
- [4] L. Hedin, *Phys. Rev.* **139**, A796 (1965).
- [5] M. Shishkin and G. Kresse, *Phys. Rev. B* **74**, 035101 (2006).
- [6] H. Peng, M. Wang, M. Wu, J. Shi, and B. F. Chen, *Phys. Rev. B* **94**, 245418 (2016).
- [7] H. Peng, M. Wang, M. Wu, J. Shi, and B. F. Chen, *Phys. Rev. B* **94**, 245418 (2016).
- [8] P. Deák, B. Aradi, and T. Frauenheim, *Phys. Rev. B* **83**, 155207 (2011).
- [9] H. Peng and S. Lany, *Phys. Rev. B* **85**, 201202 (2012).
- [10] L. Stephan, *J. Phys. Condens. Matter.* **27**, 283203 (2015).
- [11] S. L. Dudarev, G. A. Botton, S. Y. Savrasov, C. J. Humphreys, and A. P. Sutton, *Phys. Rev. B* **57**, 1505 (1998).
- [12] S. Lany, H. Raebiger, and A. Zunger, *Phys. Rev. B* **77**, 241201 (2008).
- [13] S. Lany and A. Zunger, *Phys. Rev. B* **78**, 235104 (2008).
- [14] M. Gajdoš, K. Hummer, G. Kresse, J. Furthmüller, and F. Bechstedt, *Phys. Rev. B* **73**, 045112 (2006).
- [15] J. S. Helton, K. Matan, M. P. Shores, E. A. Nytko, B. M. Bartlett, Y. Yoshida, Y. Takano, A. Suslov, Y. Qiu, J. H. Chung *et al.*, *Phys. Rev. Lett.* **98**, 107204

- [16] C. M. Pasco, B. A. Trump, T. T. Tran, Z. A. Kelly, C. Hoffmann, I. Heinmaa, R. Stern, and T. M. McQueen, *Phys. Rev. Mater.* **2**, 044406 (2018).
- [17] T.-H. Han, J. Singleton, and J. A. Schlueter, *Phys. Rev. Lett.* **113**, 227203 (2014).
- [18] Y. Tokura, H. Takagi, and S. Uchida, *Nature* **337**, 345 (1989).
- [19] H. Takagi, S. Uchida, and Y. Tokura, *Phys. Rev. Lett.* **62**, 1197 (1989).